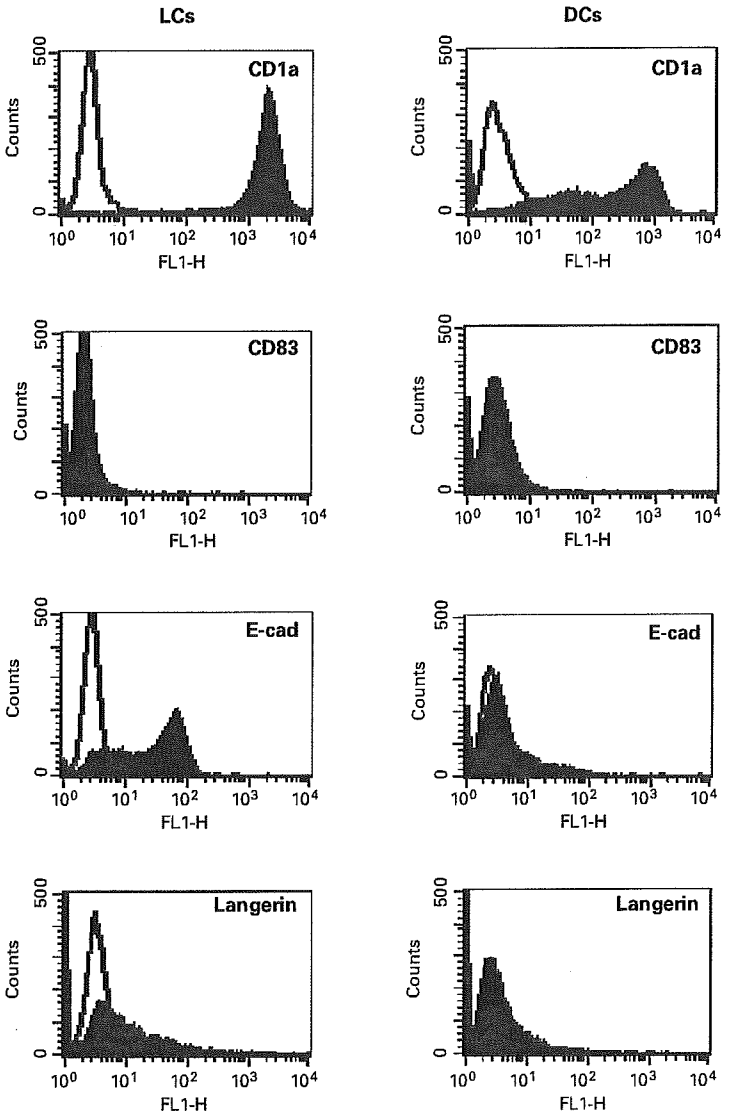

Fig. 1. Flow cytometric analysis of specific molecule expression on LCs (left panels) and DCs (right panels). LCs and DCs were generated from human PBMCs in the presence of GM-CSF, IL-4 and TGF-β1 or GM-CSF and IL-4, respectively, as described in the Materials and Methods. On day 6, cultured cells were stained with either anti-CD1a, E-cadherin, CD83, or Langerin-specific mAb and the labeled cells (1×10^4) were analyzed with a FACScan using CellQuest software. The unfilled line indicates the isotype-matched negative control.

Protein Synthesis in Immature DCs and LCs Infected with MV

Next, to study the intracellular protein synthesis in DCs and LCs infected with MV, we examined the contents of NP protein in the lysate of infected cells by Western blot analysis. As shown in the upper and the lower corresponding panels of figure 5, NP protein was observed in both immature DCs and cfgLCs but not in immature LCs. Moreover, the protein synthesis was markedly enhanced in the mechanically stimulated DCs by centrifugation (cfgDCs) when they were infected with MV.

Proliferating Response of Peripheral Blood T Cells to LCs

Finally, we examined whether those MV-treated cells maintained their immunological functions as APC, by

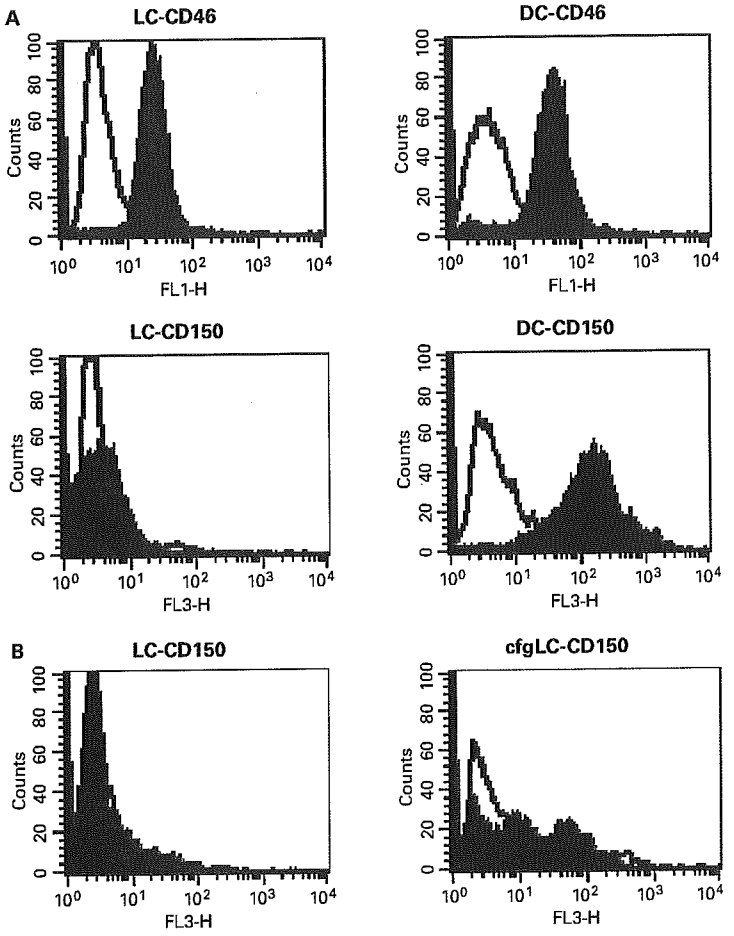

Fig. 2. Expression of the MV receptor on LCs using mAbs against CD46 and CD150. **A** LCs were treated with either anti-CD46, anti-CD150 (filled part) or control IgG (thick line). Labeled cells (1×10^4) were analyzed by a FACScan using CellQuest software. **B** After 6 days of culturing, cells were resuspended in either 48-well or 96-well culture plates at 5×10^5 cell/ml in complete medium supplement. Then, the cells were further incubated for an additional 48 h with GM-CSF, IL-4, and TGF-β1. After being cultured for 2 days, LCs were stained with anti-CD150 mAb.

testing their ability to induce the proliferation for allogeneic peripheral blood T cells. Initial experiments using this system yielded equivalent results to those obtained by [^{3}H]thymidine incorporation. As shown in figure 6, T cell proliferation was observed in response to both LCs and cfgLCs, while cfgLCs infected with MV markedly suppressed the proliferation of naive T cells in allo-MLR. However, as expected, MV-pulsed LCs did not show any measurable reduction for allo-MLR, again indicating that without centrifugation LCs would not be infected with MV, which was also confirmed by fusion formation (fig. 6).

Discussion

The present study showed that MV did not replicate in PBMC-derived unstimulated LCs that express CD1a, E-cadherin and Langerin, but not CD83, although the PBMC-derived unstimulated DCs were highly susceptible to the MV infection. In addition, the expression of CD150, a receptor for MV, was not detected on the surface of the unstimulated LCs. Nevertheless, we observed that the PBMC-derived LCs became susceptible to MV infection to form syncytia, when they were stimulated by mechanical stress such as washing and centrifugation (cfgLCs). Also, we could detect the CD150 molecules on the surface of those stimulated cfgLCs.

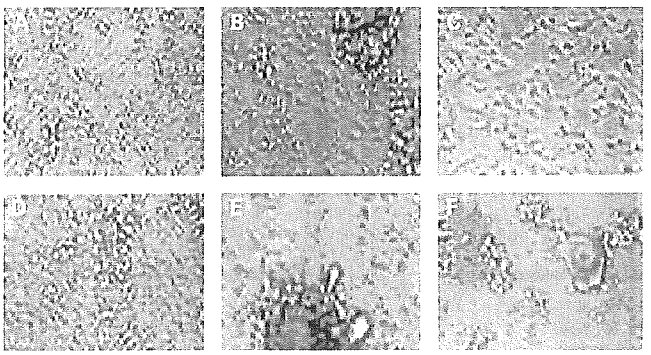

Fig. 3. Syncytia formation induced by MV infection in cultured DCs or LCs. On day 6 of the in vitro culturing, the established LCs (**A**, **D**), DCs (**B**, **E**) and cfgLCs (**C**, **F**) were plated in 96-well culture plates at a concentration of 5×10^5 cells/ml. Then the cells were further infected with MV at MOI 0.1 (**D**, **E**, **F**) and observed syncytia formation in each well on day 3 of culturing in the presence of GM-CSF, IL-4 and TGF-β1.

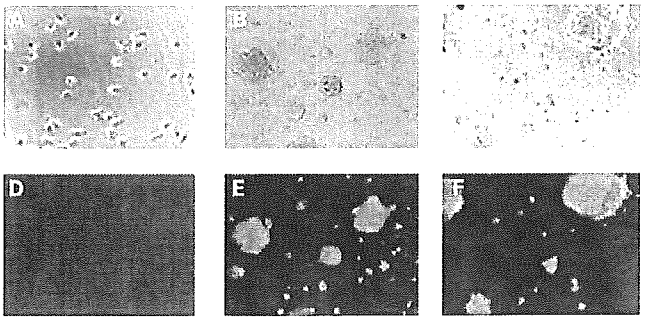

Fig. 4. Indirect immunofluorescence staining of DCs or LCs. Cells were resuspended in 96-well culture plates 5×10^5 cell/ml in complete medium supplemented with cytokines after 6 days of culture. Then, the cells were further infected with MV at MOI 0.1. Syncytia formation in LCs (**A**, **D**) and DCs (**B**, **E**) was observed on day 3 of culturing in the presence of GM-CSF, IL-4 and TGF-β1. CfgLCs (**C**, **F**) were washed three times with PBS before infection by MV. 72 h after infection, the cells were washed and stained with mAbs against MV-H protein and FITC-conjugated anti-mouse IgG (**D**, **E**, **F**).

It has been reported that freshly isolated Langerhans cells, immature DCs located in skin and mucosal epithelia, were susceptible to MV infection [4]. In that paper, centrifugation for 20 min at 1,400 rpm over a Lymphoprep gradient was carried out to obtain the Langerhans cells from the skin, which might stimulate the cells to be susceptible to MV infection. Also, those cells were probably matured by various mechanical stresses, since 61% of them had expressed CD83 molecules on their surface. Moreover, it has recently been reported that infection of the murine epidermis by herpes simplex virus did not result in the priming of virus-specific cytotoxic T lymphocytes by Langerhans, but rather that the priming response required a distinct CD8α-positive DCs [21], suggesting that epidermal Langerhans cells will not easily be infected by viruses to stimulate local immunity in the normal situation. Similarly, we have found that the responsiveness of PBMC-derived LCs to bacterial components was down-regulated in pathogen invasion in comparison with DCs to prevent local hypersensitivity [12]. Therefore, Langerhans cells seem to suppress unfavorable local responses for keeping their natural conditions although they possess a capacity to become sentinel alert cells in case they are strongly stimulated either mechanically or environmentally. For example, Langerhans cells in the skin might be activated by vigorous scratching or by high temperature. We are currently examining the effect of temperature on cytokine production and surface expression of various molecules like CD150 on the PBMC-derived LCs.

The LCs used in this study expressed CD1a, E-cadherin, and the Lag protein but not CD83. Although Birbeck granule-associated Lag antigen was stained at a level of less than 30%, we could detect Birbeck granules and observe the expression of langerin in the LCs, indicating that the obtained LCs were analogous to Langerhans cells freshly isolated from the skin. To successfully generate immature LCs that do not express CD83 from PBMCs by culturing, we have to avoid a mechanical stress as best as possible and select good batches of FCS since we sometimes detected CD83 molecules on the surface of cultured LCs when we used a distinct batch of FCS, which might be contaminated by unfavorable substances like lipopolysaccharide which will maturate the cultured LCs into CD83-positive LCs [12].

In this study, we showed that CD150, a receptor for MV infection, appeared on the surface of PBMC-derived LCs when stimulated by mechanical stress like centrifugation. Such mechanical stress is known to alter the expression of several adhesion molecules like CD150 on leukocytes [22]. In general, human leukocytes retract pseudopods in response to physiological fluid shear, a phenomenon that serves to keep circulating leukocytes in the spherical state to prevent active pseudopod formation. However, it has recently been proved that centrifugation atten-

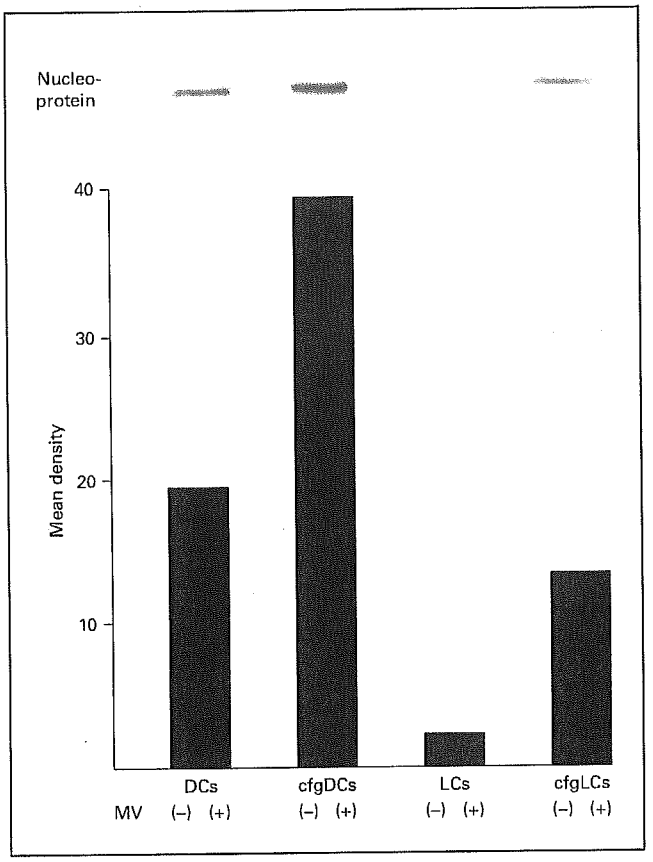

Fig. 5. Virus-associated polypeptide synthesis in DCs, cfgDCs, LCs and cfgLCs. Cells were solubilized with SDS lysis buffer at 72 h after infection and samples were analyzed by SDS-PAGE. The levels of nucleoprotein were quantified by densitometry and analyzed with NIH image software.

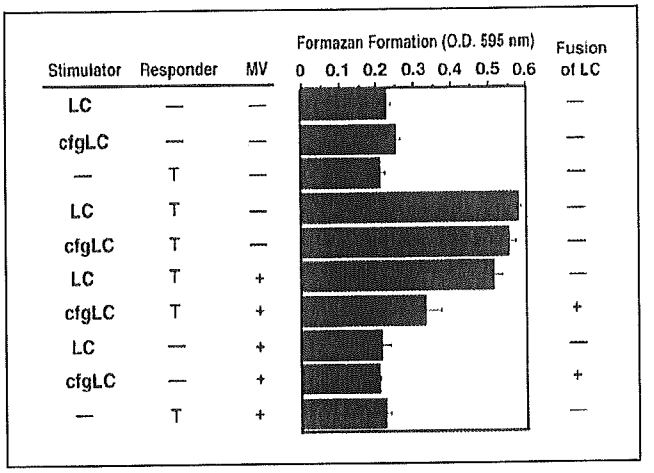

Fig. 6. Proliferative responses of peripheral blood T cells to allogeneic LCs. Nylon column-purified T cells (2×10^5/well) were stimulated with 2,500 rad-irradiated various LC preparations (5×10^3/well) in 200 µl of complete medium in 96-well U-bottom microplates for 3 days, and their proliferative responses were assessed by measuring MTT cleavage as described in Materials and Methods.

uates irreversibly the fluid shear response and stimulates the leukocytes to produce pseudopod projection instead of retraction during shear application, which can be suppressed by a calcium channel blocker, such as diltiazem, a voltage-dependent Ca^{2+} channel blocker [23]. Although it remains to be determined what kind of mechanical stress elements stimulates PBMC-derived LCs to be susceptible to MV, the Ca^{2+} channel blocker may retract the expression of CD150 and reduce the susceptibility of LCs to MV infection in vivo.

We also examined whether MV could affect the ability of LCs and cfgLCs to stimulate naive allogeneic T cells. Freshly isolated Langerhans cells from the skin strongly stimulated allogeneic peripheral blood T cells to proliferate [4]. In contrast, as shown in figure 6, PBMC-derived cfgLCs incubated with MV did block the proliferation of naive T cells in allo-MLR. This may be because the MV-infected LCs are sufficient to induce the arrest of stimulated T cell proliferation in vitro [24]. The findings strongly suggest that virus-sensitized Langerhans cells may act to suppress local immune responses initiated by virus intrusion.

In conclusion, the actual role of Langerhans cells in local immunity must be reconsidered, in that they are not the cells to stimulate local immune responses but rather cease the fire of unfavorable reactions initiated by virus intrusion as well as by dissemination of bacteria invasion [12]. However, such local sentinel Langerhans cells will have a capacity to alert immune effectors in case they are activated by vigorous local stimulation mediated through mechanical stresses such as scratches, burn and injury. Further investigation will reveal the true function of Langerhans cells against virus infection.

Acknowledgments

We thank Dr. Y. Yamaji for generously providing the Rapp clone of the Measles-Edmonston strain, and for his helpful insight. Also, we thank Dr. Junko Takeuchi for the helpful discussion. This work was supported in part by grants from the Ministry of Education, Culture and Science and the Ministry of Health, Japan.

References

1 Grosjean I, Caux C, Bella C, Berger I, Wild F, Banchereau J, Kaiserlian D: Measles virus infects human dendritic cells and blocks their allostimulatory properties for CD4+ T cells. J Exp Med 1997;186:801–812.

2 Schnorr JJ, Xanthakos S, Keikavoussi P, Kampgen E, ter-Meulen V, Schneider-Schaulies S: Induction of maturation of human blood dendritic cell precursors by measles virus is associated with immunosuppression. Proc Natl Acad Sci USA 1997;94:5326–5331.

3 Murabayashi N, Kurita-Taniguchi M, Ayata M, Matsumoto M, Ogura H, Seya T: Susceptibility of human dendritic cells (DCs) to measles virus (MV) depends on their activation stages in conjunction with the level of CDw150: Role of Toll stimulators in DC maturation and MV amplification. Microbes Infect 2002;4:785–794.

4 Steineur MP, Grosjean I, Bella C, Kaiserlian D: Langerhans cells are susceptible to measles virus infection and actively suppress T cell proliferation. Eur J Dermatol 1998;8:413–420.

5 Servet-Delprat C, Vidalain PO, Bausinger H, Manie S, Le-Deist F, Azocar O, Hanau D, Fischer A, Rabourdin-Combe C: Measles virus induces abnormal differentiation of CD40 ligand-activated human dendritic cells. J Immunol 2000;164:1753–1760.

6 Minagawa H, Tanaka K, Ono N, Tatsuo H, Yanagi Y: Induction of the measles virus receptor SLAM (CD150) on monocytes. J Gen Virol 2001;82:2913–2917.

7 Geissmann F, Revy P, Regnault A, Lepelletier Y, Dy M, Brousse N, Amigorena S, Hermine O, Durandy A: TGF-beta 1 prevents the noncognate maturation of human dendritic Langerhans cells. J Immunol 1999;162:4567–4575.

8 Bell D, Young JW, Banchereau J: Dendritic cells. Adv Immunol 1999;72:255–324.

9 Banchereau J, Steinman RM: Dendritic cells and the control of immunity. Nature 1998;392:245–252.

10 Merad M, Manz MG, Karsunky H, Wagers A, Peters W, Charo I, Weissman IL, Cyster JG, Engleman EG: Langerhans cells renew in the skin throughout life under steady-state conditions. Nat Immunol 2002;3:1135–1141.

11 Geissmann F, Dieu-Nosjean MC, Dezutter C, Valladeau J, Kayal S, Leborgne M, Brousse N, Saeland S, Davoust J: Accumulation of immature Langerhans cells in human lymph nodes draining chronically inflamed skin. J Exp Med 2002;196:417–430.

12 Takeuchi J, Watari E, Shinya E, Norose Y, Matsumoto M, Seya T, Sugita M, Kawana S, Takahashi H: Down-regulation of Toll-like receptor expression in monocyte-derived Langerhans cell-like cells: Implications of low responsiveness to bacterial components in the epidermal Langerhans cells. Biochem Biophys Res Commun 2003;306:674–679.

13 Takahashi M, Osono E, Nakagawa Y, Wang J, Berzofsky JA, Margulies DH, Takahashi H: Rapid induction of apoptosis in CD8+ HIV-1 envelope-specific murine CTLs by short exposure to antigenic peptide. J Immunol 2002;169:6588–6593.

14 Geissmann F, Prost C, Monnet JP, Dy M, Brousse N, Hermine O: Transforming growth factor beta1, in the presence of granulocyte/macrophage colony-stimulating factor and interleukin 4, induces differentiation of human peripheral blood monocytes into dendritic Langerhans cells. J Exp Med 1998;187:961–966.

15 Rapp F: Plaque differentiation and replication of virulent and attenuated strains of measles virus. J Bacteriol 1964;88:1448–1458.

16 Reed LJ, Muench H: A simple method of estimating fifty percent endpoints. Am J Hyg 1938;27:493–497.

17 Watari E, Shinya E, Kurane S, Takahashi H: Effects of cyclosporin A on cell fusion in a monkey kidney cell line persistently infected with measles virus. Intervirol 2001;44:209–214.

18 Laemmli UK: Cleavage of structual proteins during the assembly of the head of bacteriophage T4. Nature 1970;227:680–685.

19 Kemper C, Chan AC, Green JM, Brett KA, Murphy KM, Atkinson JP: Activation of human CD4+ cells with CD3 and CD46 induces a T-regulatory cell 1 phenotype. Nature 2003;421:388–392.

20 Heeg K, Reimann J, Kabelitz D, Hardt C, Wagner H: A rapid colorimetric assay for the determination of IL-2-producing helper T cell frequencies. J Immunol Methods 1985;77:237–246.

21 Allan RS, Smith CM, Belz GT, van Lint AL, Wakim LM, Heath WR, Carbone FR: Epidermal viral immunity induced by CD8alpha+ dendritic cells but not by Langerhans cells. Science 2003;301:1925–1928.

22 Lundahl J, Hallden G, Hallgren M, Skold CM, Hed J: Altered expression of CD11b/CD18 and CD62L on human monocytes after cell preparation procedures. J Immunol Methods 1995;180:93–100.

23 Fukuda S, Schmid-Schonbein GW: Centrifugation attenuates the fluid shear response of circulating leukocytes. J Leukoc Biol 2002;72:133–139.

24 Schlender J, Schnorr JJ, Spielhoffer P, Cathomen T, Cattaneo R, Billeter MA, ter Meulen V, Schneider-Schaulies S: Interaction of measles virus glycoproteins with the surface of uninfected peripheral blood lymphocytes induces immunosuppression in vitro. Proc Natl Acad Sci USA 1996;93:13194–13199.

Tissue Antigens ISSN 0001-2815

Analysis of evolutionary conservation in CD1d molecules among primates

N. Saito[1,2], M. Takahashi[1,3], W. Akahata[2], E. Ido[2], C. Hidaka[3], K. Ibuki[2], T. Miura[2], M. Hayami[2] & H. Takahashi[1,3]

1 Laboratory of Virus Control, Institute for Virus Research, Kyoto University, 53 Shogoin-Kawahara-cho, Kyoto 606-8507, Japan
2 Laboratory of Primate Model, Institute for Virus Research, Kyoto University, 53 Shogoin-Kawahara-cho, Kyoto 606-8507, Japan
3 Department of Microbiology and Immunology, Nippon Medical School, 1-1-5, Sendagi, Bunkyo-ku, Tokyo 113-8602, Japan

Key words
African green monkey; CD1d; chimpanzee; HIV-1/ SIV; NKT; primate; rhesus monkey; susceptibility

Correspondence
Hidemi Takahashi, MD, PhD
Department of Microbiology and Immunology
Nippon Medical School
1-1-5, Sendagi, Bunkyo-ku
Tokyo 113-8602, Japan
Tel: 81 3 3822 2131x5381
Fax: 81 3 3316 1904
e-mail: htkuhkai@nms.ac.jp

Received 15 June 2005; revised 15 August 2005; re-revised 28 August 2005; accepted 2 September 2005

doi: 10.1111/j.1399-0039.2005.00504.x

Abstract

The hereditary conservation in the genetically encoded *CD1D* sequences of various primates was analyzed. Genomic *CD1D* sequences of 17 rhesus macaques with distinct origins, eight Indian and nine Chinese, were examined and differences of only one or two nucleotides were detected and the consensus sequence of rhesus *CD1D* was determined. *CD1D* consensus sequences of three African green monkeys (AGMs) and the rhesus monkeys were then compared to study the evolutionary differences among interspecies. The *CD1D* consensus sequence determined from AGMs apparently differed by seven nucleotides from the rhesus consensus sequence, and nucleotide difference induced only three amino acid changes within Exon3, corresponding to the α_2 domain of CD1d having a hydrophobic ligand-binding pocket. Such changes in the α_2 domain may alter the characteristics of the SIV-derived glycolipid/lipid antigens presented by each CD1d molecule to innate natural killer T cells. In addition, the *CD1D* genomic sequences of three chimpanzees (chimps) were determined. To our surprise, although Exon2 and Exon3 reflecting antigen-binding α_1 and α_2 domains in chimps' *CD1D* were identical to that in humans except one amino acid, three amino acids within Exon4, reflecting α_3 domain, were distinct from humans, and one of them was identical to those in rhesus and AGM *CD1D*. On the basis of the findings, the evolutionary relationship of the CD1d molecules among the various primates and their HIV-1/SIV susceptibility will be discussed.

Introduction

Unlike B lymphocytes bearing immunoglobulin receptors that can bind directly onto various free antigens, T lymphocytes can recognize foreign antigens as their processed fragments in conjunction with antigen-presenting molecules on the surface of antigen-presenting cells (APCs) (1). Such antigen-presenting molecules are usually classified into three groups: class I major histocompatibility complex (MHC), class II MHC, and CD1. The first two MHC molecules can present processed peptide antigens, whereas the last CD1 can present glycolipid/lipid antigens derived from various pathogens (2). In general, endogenously synthesized foreign antigens such as viral proteins are degraded into peptide fragments composed of eight to 10 amino acids in the cytosol through an ATP-dependent proteolytic system, trapped into the class I MHC groove and presented to specific $CD8^+$ T lymphocytes (3). In contrast, free soluble and particulate peptide antigens from various pathogens are captured exogenously by APCs such as immature dendritic cells (iDCs), transported to acidic endosomal compartment, where the captured antigens are further degraded to fit into the channel of class II MHC, and the peptide-loaded class II MHC molecules are exported to the cell surface for the stimulation of antigen-specific $CD4^+$ T lymphocytes (4).

As for CD1 antigen presentation, there have been four distinct types of CD1 molecules (CD1a, b, c, and d) identified on the surface of human APCs, and two subclasses

of CD1d are found in mice to present glycolipid/lipid but not conventional processed peptide antigens (5, 6). On the basis of sequence homologies, these CD1 molecules can be classified into two types: CD1a, b, and c as group 1 and CD1d as group 2 (7). These CD1 molecules present unique glycolipid/lipid antigens with amphipathic structure whose hydrophobic lipid tails are bound to deep cavity in the CD1s and present lipid–sugar complex to T cells expressing αβ T-cell receptors (TCRs). For example, CD1a presents dideoxymycobactin (DDM) (8), CD1b lipoarabinomannan (LAM) (9), glucose monomycolate (GMM) (10), and mycolic acid (11); CD1c mannosyl phosphoisoprenoid (12) and CD1d glycosyl-phosphatidyl inositol (GPI) (13); or α-galactosyl ceramide (αGalCer) (14). Such glycolipid/lipid antigens presented by the group 1 CD1 molecule (CD1a, b, and c) on DCs stimulate conventional αβ TCR-bearing T cells expressing either $CD8^+$ T cells or $CD4^-CD8^-$ T cells, whereas antigens presented by group 2 CD1 (CD1d) on DCs, as well as various types of mononuclear cells, such as T cells, B cells, and monocytes, activate natural killer T (NKT) cells. NKT cells are a subset of T cells expressing not only NK receptor but also invariant αβ TCRs such as Vα24 TCR in humans (15) and Vα14 in mice (16) for the recognition of glycolipid/lipid antigens like αGalCer presented by the CD1d.

The structures of these CD1 molecules are similar to those of class I MHCs bearing noncovalently bound β_2 microglobulin; however, the CD1s show limited polymorphism and do not map to the MHC genes (17). Moreover, although class I and II MHC molecules are extremely diverse among species with self-restricted elements that can present processed antigens only to the same MHC-bearing cells, the CD1-encoding genes are highly conserved, and their structures are shared among species (18), indicating the importance of CD1-restricted effectors for maintaining species evolution, and mutation or inactivation of the CD1s might deprive the species continuity. Furthermore, the fact that mice and rats have only CD1d among other classical CD1s in a highly conserved manner (19) reveals that the preservation of CD1d molecules together with NKT cells as their evolutionarily selected partners seems to be critical for such rodents to evolve.

In the present study, we focused on analyzing the hereditary conservation in the genetically encoding *CD1D* sequences of various primates. To date, human and rodent *CD1D* sequences (20–22) and some portion of genomic DNA of rhesus macaque have been reported (23). Therefore, we first confirmed whether the genomic DNA sequence of *CD1D* was identical to the cDNA encoding *CD1D* message by establishing iDCs from peripheral blood mononuclear cells (PBMCs) of rhesus macaques to determine the *CD1D* consensus sequence. We then compared the *CD1D* sequences of African green monkeys (AGMs) and rhesus monkeys to see the evolutionary difference in the CD1d molecules among interspecies. Finally, we determined for the first time the genomic sequences of *CD1D* in chimpanzees (chimps) for comparison. On the basis of the findings obtained here, the evolutionary relationship in the CD1d molecules among various primates and their HIV-1/SIV susceptibility as models for HIV-1 infection will be discussed.

Materials and methods

Animals

Seventeen rhesus macaques (*Macaca mulatta*), nine Chinese originated and eight Indian originated, and three AGMs (*Cercopithecus aetiops grivet*) were used in this experiment. All monkeys used in this study were housed in accordance with regulations approved by the Institutional Animal Care and Use Committee of the Institute for Virus Research, Kyoto University. Three blood samples of chimps (*Pan troglodytes*) were kindly obtained from Dr S. Singh (Cornell University).

Induction of iDCs from PBMCs

PBMCs of rhesus macaques were isolated from heparinized blood by density gradient centrifugation using Lymphocyte Separation Solution (Nakarai Tesque, Kyoto, Japan) and cultured in monocyte-separating plates (MSP-P) (JIMRO, Gunma, Japan) at 1×10^7 cells in 2.5 ml of Dulbecco's modified Eagle medium (DMEM) (Gibco-BRL, Grand Island, NY), supplemented with 10% fetal calf serum (FCS) for 1–2 h in a 5% CO_2 incubator at 37°C as described recently (24). After incubation, the non-adherent cells were removed, and the adherent monocytes were further cultured in 2.5 ml DMEM supplemented with 10% FCS, 200 ng/ml recombinant human granulocyte macrophage-colony-stimulating factor (rhGM-CSF) (R&D system, Minneapolis, MN), and 50 ng/ml recombinant human interleukin-4 (rhIL-4) (R&D system) for an additional 6–8 days to generate the CD1-expressing monocyte-derived iDCs as described previously (25).

RNA extraction from rhesus iDCs and cDNA synthesis

RNAs were extracted from the established monocyte-derived iDCs using total RNA isolation reagent for the liquid samples (TRIZOL; Gibco-BRL). Then poly-A-tailed mRNAs were collected from the extracted total RNA and changed into cDNA with a first-strand cDNA Synthesis Kit (Invitrogen, Carlsbad, CA).

Cloning of *CD1D*-encoding genes

Preparation of PCR product

In order to proceed with the cloning of rhesus *CD1D* genes, the cDNA obtained was added to a mixture

containing 10 mM Tris–HCl (pH 8.3), 50 mM KCl, 2.5 mM $MgCl_2$, 200 μM of each dNTPs, 0.2 μM of each primer, and 2.5 units of AmpliTaq DNA polymerase (Roche Diagnostics GmbH, Mannheim, Germany). The amplification of cDNA fragments was performed for 35 cycles consisting of the following three steps: denaturation at 94°C for 60 s (5 min for the first cycle), annealing at 55°C for 60 s, and elongation at 72°C for 90 s (5 min for the last cycle). The primers shown below were estimated on the basis of human *CD1D* sequences (26): CD1d (forward) (5′-TTCACA GGACGCCCTGATAGGAACTTTGCCTCTTAAACC-GGGAGGTAAAGCCCAC-3′) and CD1d (reverse) (5′-TCAGGACGCCCTGATAGGAACTTTGCCTCTTAA-ACCGGGAGGTAAAGCCCAC-3′).

Subcloning of PCR product

The PCR products were then run in a 1.5% agarose gel supplemented with ethidium bromide. The specified bands were excised and purified using a QIAquick Gel Extraction Kit (Qiagen, Valencia, CA). Purified cDNAs were ligated into a pCR2.1-TOPO TA cloning vector (Invitrogen) and inserted into their competent cells (*Escherichia coli*-derived DH5α; Invitrogen). After 24 h incubation, white colonies were picked for sequencing experiments. Twelve white colonies from LB plate were picked up and the sequence analysis was performed on four clones. Three sequencing experiments were carried out to account for false positive.

Sequence analysis of cloned cDNA

Sequence analysis was performed using a DNA sequencing Kit (Big Dye Terminator Cycle Sequencing Ready Reaction; Applied Biosystems, Foster city, CA). The amplification of cDNA fragments was performed for 25 cycles, consisting of denaturation at 96°C for 10 s, annealing at 50°C for 5 s, and elongation at 60°C for 4 min. Sequences of amplified DNA fragments were determined with an ABI PRISM 3100 Genetic Analyzer (Applied Biosystems). M13 primers were used for sequencing analysis: M13 (forward) (5′-GTAAAACGACGGCCAG-3′) and M13 (reverse) (5′-CAGGAAACAGCTATGAC-3′).

Direct sequencing of *CD1D* from genomic DNA

Genomic DNA was extracted from PBMCs of various primates with QIAamp DNA Mini Kit (Qiagen GmbH, Hilden, Germany). Then the genomic DNA was subjected to the PCR. The following primers were prepared on the basis of human genomic *CD1D* sequence (26):

Exon1	E1F	(5′-AGAAGAGTGCGCAGGTCAGAGG GCGGCCGC-3′)
	E1R	(5′-CGCCAGTGCGTCCCGGGTCTCAC CAGT CCC-3′)
Exon2	E2F	(5′-ATGCTGGCTGCTCTCCCGGCC ACTTGCTAC-3′)
	E2R	(5′-TCTGTGGCCATTCTCTCCCCTT GGGTAC CG-3′)
Exon3	E3F	(5′-TCTCTTTCATCTCTCCCAGTCT TTTAAAC-3′)
	E3R	(5′-GGAAAAGCCCGTTTGGAGCCC TGAAG TGGA-3′)
Exon4	E4F	(5′-GGAGCCTCTAATGCAGAGTTT TCACTTTAA-3′)
	E4R	(5′-CACCCCAGTGCCTCCCTCTAT GCCTGA GGA-3′)
Exon5–6	E5F	(5′-ATTGGGGTTTTAAGTGGAG GAGGAAATAAG-3′)
	E5R	(5′-TTTCAAGGTATCTCTCCTATCT TCAATT CC-3′)

The amplification of DNA fragments was performed for 35 cycles, consisting of denaturation at 94°C for 30 s (5 min for the first cycle), annealing at 60°C for 30 s, and elongation at 72°C for 45 s (5 min for the last cycle) and confirmed with agarose gel electrophoresis. The DNA fragments were purified and then analyzed with an ABI PRISM 3100 Genetic Analyzer. In the case of the thin fragments, they were ligated into the TA cloning site of pCR 2.1-TOPO Vector (TOPO TA Cloning; Invitrogen) and inserted into their competent cells (*Escherichia coli*-derived DH5α; Gibco-BRL). The plasmid was prepared by the alkaline lysis method (27), and the purified plasmid was used for sequence analysis.

GenBank accession

Each determined sequence of the *CD1D* was submitted to public database and obtained the GenBank accession numbers as follows:

C-1 to C-7 and C-9 are corresponding to the numbers of AB222829 to AB222836, respectively, and C-8 is to AB232047. I-1 to I-8 are corresponding to the numbers of AB222837 to AB222844, respectively. Three AGMs are corresponding to the numbers of AB222994 to AB222996 and three chimps are to AB222997, AB222998, and AB223044, respectively.

Results

Establishment of iDCs from PBMCs of a rhesus macaques and the cloning and sequencing of their CD1d molecules

Because CD1d molecules are generally expressed on DCs or iDCs, we first established the iDCs from freshly isolated PBMCs of a rhesus macaque named MM257 by culturing them with GM-CSF and rhIL-4, as previously indicated. Then, total RNA was extracted from those iDCs, and the cDNA of *CD1D* was cloned from the mRNA using reverse

transcriptase. As shown in Figure 1, the size of rhesus *CD1D* cDNA was 1014 bp, similar to that of human *CD1D* that has been reported previously (26). The cloned cDNA was inserted into competent cells for sequence analysis using a TA-cloning vector. Consequently, we obtained four clones, and their sequences were analyzed using a Genetic Sequencing Analyzer. As represented in Figure 2, we managed to determine the *CD1D* sequence of rhesus MM257. However, since only human GM-CSF and IL-4 were available to induce DCs from various primates, we have experienced serious difficulty in establishing primates' DCs from PBMCs. We thus attempted to confirm whether the genomic DNA sequence for *CD1D* was similar to the *CD1D* message encoded in the cDNA to determine the *CD1D* consensus sequence and found that both sequences were identical in the rhesus MM257 (data not shown). Therefore, we examined the genomic DNA instead of the mRNA-derived cDNA for further analysis.

Comparison of *CD1D* sequences among rhesus macaques with distinct origins

In contrast to class I and class II MHC molecules composed of distinct sequences of amino acids in each individual even among the same species, CD1 molecules consist of species-specific and highly conserved sequences (22). Therefore, we speculated that the *CD1D* sequence of MM257 would probably be the same as other rhesus macaques. We examined the genomic *CD1D* sequences of 16 additional rhesus macaques. The former eight macaques originated from China including MM257 and the latter eight were from India. As expected, in comparison with the whole *CD1D* sequences of MM257, only one or two nucleotide differences could be found among other samples, and the consensus sequence of the rhesus *CD1D* was determined from the results (Table 1). Since these nucleotide changes affected only one amino acid alteration

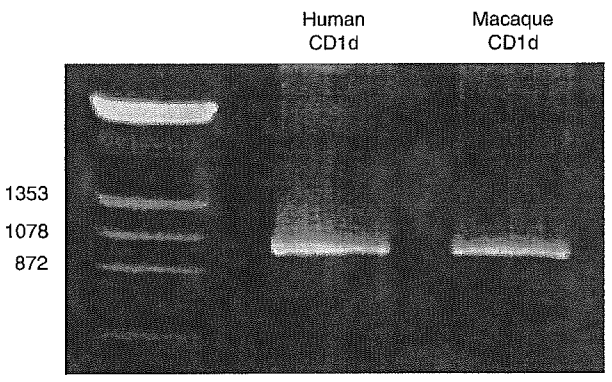

Figure 1 Amplification of the rhesus macaque *CD1D* cDNA from monocyte-derived immature dendritic cells. The size of specific band (bp) obtained by RT-PCR was similar to that of human CD1d.

at position 896, Leu for MM257 and His for other monkeys in Exon5, such changes do not have an influence on antigen presentation by CD1d molecules (28).

Comparison of *CD1D* sequences between rhesus macaques and AGMs

Because the susceptibility to SIV is totally different between rhesus macaques and AGMs in that the rhesus macaques will develop immune-deficient states with marked decrease in CD4, whereas the latter AGMs will not, although AGMs have been thought as natural hosts of SIV (29); we examined whether the *CD1D* sequences were genetically conserved between those species. As shown in Table 2, the consensus *CD1D* sequence determined from the AGMs differed by seven nucleotides from the rhesus consensus sequence. Nevertheless, these nucleotide differences resulted in three amino acid changes within Exon3, corresponding to the α_2 domain of CD1d, having a hydrophobic ligand-binding pocket (28).

Comparison of the consensus *CD1D* sequences of rhesus macaques and AGMs with those of chimps and humans

These rhesus macaques and AGMs are not susceptible to HIV-1, but both chimps and humans are susceptible to HIV-1, but not to SIV (30). We thus conducted direct sequencing for *CD1D* using PBMCs obtained from three chimps (kindly provided by Dr S. Singh, Cornell University) to determine the consensus *CD1D* sequence of chimps. Nucleotide sequences (Figure 3A) and amino acid alignments (Figure 3B) among humans, chimps, rhesus macaques, and AGMs are summarized. Unexpectedly, both Exon2 and Exon3, reflecting the antigen-binding sites of the α_1 and α_2 domains, were identical except for one amino acid, Glu(E), at position 182 between chimps and humans. However, three amino acids, Asp (D), Ala (A), and Ile (I), at positions 229, 252, and 274 within Exon4, reflecting α_3 domain, were distinct from humans, and one of them was identical to those in rhesus and AGM *CD1D*. Moreover, on the basis of recent reports on the precise structural analysis of CD1d molecules for antigen presentation to NKT cells (31–34), we boxed the amino acid sequences crucial for antigen presentation and highlighted the amino acids critical for human NKT-cell activation among them (Figure 3B).

Discussion

In the present study, we first determined the *CD1D* sequence of a rhesus macaque, named MM257, from mRNA-derived cDNA clones and confirmed the consistency of the sequence with genomic DNA obtained from MM257 PBMC to decide the consensus sequence. We then

```
        10         20         30         40         50         60         70         80         90        100        110        120
ATGGGGTGCCTGCTGTTTCTGCTGCTCTGGGCGCTCCTCCAGGCTTGGGGAAGCGCTGAAGTCCCGCAAAGGCTTTTCCCCCTCCGCTGCCTCCAAATCTCGTCCTTCGCCAATAGCAAC
M  G  C  L  L  F  L  L  L  W  A  L  L  Q  A  W  G  S  A  E  V  P  Q  R  L  F  P  L  R  C  L  Q  I  S  S  F  A  N  S  N

       130        140        150        160        170        180        190        200        210        220        230        240
TGGACGCGCACCGATGGTTTGGCGTGGCTGGGGGAGCTGCAGACGCACAGCTGGAGCAACGACTCCGACACCATCCGCTCTCTGAAGCCGTGGTCCCAGGGCACGTTCAGCGACCAGCAG
W  T  R  T  D  G  L  A  W  L  G  E  L  Q  T  H  S  W  S  N  D  S  D  T  I  R  S  L  K  P  W  S  Q  G  T  F  S  D  Q  Q

       250        260        270        280        290        300        310        320        330        340        350        360
TGGGAGGCGCTGCAGCGTGTATTTCGGGTTTATCGAAGCAGCTTCACCAGGGACGTGAAGGAATTCGCCAAAATGCTGCGCTTAGCCTATCCCATGGAGCTCCAGGTGTCTGCTGGCTGT
W  E  A  L  Q  R  V  F  R  V  Y  R  S  S  F  T  R  D  V  K  E  F  A  K  M  L  R  L  A  Y  P  M  E  L  Q  V  S  A  G  C

       370        380        390        400        410        420        430        440        450        460        470        480
GAGGTGCACCCTGGAAACGCCTCACATAACTTCTTCCATGTAGCGTTTCAAGGAAGTGATATCCTGAGTTTCCAAGGAACTTCTTGGGAACCAGCCCAAGAGGCCCCACTTTGGGTAAAC
E  V  H  P  G  N  A  S  H  N  F  F  H  V  A  F  Q  G  S  D  I  L  S  F  Q  G  T  S  W  E  P  A  Q  E  A  P  L  W  V  N

       490        500        510        520        530        540        550        560        570        580        590        600
TTGGCCATCCAAGTGCTCAACCAGGACAACTGGACGAAGGAAACAGTGCAGTGGCTCCTTAATGACACCTGCCCCCAATTTGTCAGTGGCCTCCTTGAGTCAGGGAAGTCGGAACTGGAG
L  A  I  Q  V  L  N  Q  D  N  W  T  K  E  T  V  Q  W  L  L  N  D  T  C  P  Q  F  V  S  G  L  L  E  S  G  K  S  E  L  E

       610        620        630        640        650        660        670        680        690        700        710        720
AAGCAAGTGAAGCCCAAGGCCTGGCTGTCCCGTGGCCCCAGTCCTGGCCCTGGCCGTCTGCAGCTTGTGTGCCATGTCTCAGGATTCTACCCAAAGCCCGTGTGGGTGAAGTGGATGCGG
K  Q  V  K  P  K  A  W  L  S  R  G  P  S  P  G  P  G  R  L  Q  L  V  C  H  V  S  G  F  Y  P  K  P  V  W  V  K  W  M  R

       730        740        750        760        770        780        790        800        810        820        830        840
GGTGAGCAGGAGCAGCAGGGCACTCAGCGAGGGGACATCCTGCCCAATGCTGACGAGACATGGTATCTCCGAGCAACCCTGGAGGTGGCCGCTGGGGAGGCAGCTGGCCTGTCCTGTCGG
G  E  Q  E  Q  Q  G  T  Q  R  G  D  I  L  P  N  A  D  E  T  W  Y  L  R  A  T  L  E  V  A  A  G  E  A  A  G  L  S  C  R

       850        860        870        880        890        900        910        920        930        940        950        960
GTGAAGCACAGCAGTCTAGAGGGCCAGGACATCGTCCTCTACTGGGGTGGGAGCCTCACCTCCGTGGGCTTGATCGCCTTGGCAGTCCTGGCATGCTTGCTGTTCCTCCTTGCACTCATT
V  K  H  S  S  L  E  G  Q  D  I  V  L  Y  W  G  G  S  L  T  S  V  G  L  I  A  L  A  V  L  A  C  L  L  F  L  L  A  L  I

       970        980        990       1000       1010       1020
GTAGGCTTTACCTTCCGGTTTAAGAGGCAAACTTCCTATCAGGGCATCCTGTGA
V  G  F  T  F  R  F  K  R  Q  T  S  Y  Q  G  I  L  *
```

Figure 2 Nucleotide and amino acid sequences of the CD1d molecule for rhesus MM257. PCR product obtained from cDNA of MM257 was inserted into a TA cloning vector and sequenced using a DNA sequencer. Analysis of the sequences was performed by GENETYX-MAC software.

Table 1 Comparison of the *CD1D* nucleotide sequences in rhesus macaques of distinct origins

Chinese										
Position (bp)	Genomic region	C-1[a]	C-2	C-3	C-4	C-5	C-6	C-7	C-8	C-9	Consensus
96	Exon2	A		G				A/G		A/G	A
199		T	C								T
450	Exon3	A		A/G	A/G	A/G	G	A/G	A/G	G	A/G
510		C			G					C/G	C
555		C			C/T					C/T	C
896	Exon5	T	A	A	A	A	A	A	A	A	A

Indian										
Position (bp)	Genomic region	I-1	I-2	I-3	I-4	I-5	I-6	I-7	I-8	Consensus
96	Exon2	A				G	A/G	A/G	G	A
199		T	A/T		C/T					T
331	Exon3	C		C/T		C/T	C/T		T	C
443		C	A/C		A/C					C
450		A/G		G	G		G		G	A/G
510		C			C/G		A/G	C/G		C
555		C			C/T		C/T	C/T		C
659	Exon4	T			G					T
838		C			C/T		C/T	C/T		C

Genomic *CD1D* sequences of 17 rhesus macaques, nine Chinese (C-1 to C-9), and eight Indian (I-1 to I-8) origins were examined, and the consensus sequence of the *CD1D* for rhesus macaques was determined.

[a] C-1 corresponds to MM257 in the text.

Table 2 Comparison of the consensus *CD1D* sequences between rhesus macaques and African green monkeys (AGMs)

		Nucleotide		Amino acid	
Position (bp)	Genomic region	AGM consensus	Macaque consensus	AGM consensus	Macaque consensus
93	Exon2	T	C	L	L
96		G	A	Q	Q
210		T	G	P	P
351	Exon3	C	T	S	S
417		A	T	**R**	**S**
510		G	C	**K**	**N**
518		G	A	**R**	**K**

Consensus sequence of the *CD1D* for AGM was determined from three monkeys. Distinct positions for each specific nucleotide and amino acid were shown. Although the consensus *CD1D* sequence of AGMs differed by seven nucleotides from the rhesus consensus sequence, these nucleotide differences induced only three amino acid changes within Exon3 (indicated as bold).

examined the genomic DNA of another 16 macaques with distinct origins and found that the *CD1D* sequence of all the monkeys tested was identical except one amino acid in Exon5. Thus, genetic structure of species-specific CD1d molecules was far more tightly conserved than that expected among the rhesus macaques and would not be affected by long-term environmental stimulation. Also, the results suggest that the mutation of the *CD1D* genes might ruin the species and indicate the importance of the CD1d-restricted NKT-related immunity for species survival. Indeed, we have recently found that the syngeneic thymoma cells were deleted by NKT-like cells when they expressed unfavorable encoding genes such as alpha-fetoprotein (35) and that dysfunction of NKT cells causes autoimmune disorders (36) or deficiencies of CD1d seems to be associated with the impairment of various infectious diseases (37) that might correlate with the disappearance of the primates bearing mutated *CD1D*.

We next examined whether the *CD1D* sequences were genetically conserved between the two distinct types of monkeys, rhesus macaques and AGMs, and found that the *CD1D* consensus sequence determined from the AGMs differed by seven nucleotides from the consensus sequence of rhesus macaques, and those nucleotide differences generated three amino acids changes within Exon3. Because Exon3 corresponds to the α_2 domain of the CD1d molecules having a hydrophobic ligand-binding pocket critical for antigen presentation (28), these changes of the amino acids may alter the capacity of the presented glycolipid/lipid antigens to effector NKT cells. In the case of SIV infection, such changes in the α_2 domain may affect the characteristics of the SIV-derived glycolipid/lipid antigens presented by the CD1d and may induce functional differences of the activated NKT cells that may result in the distinct susceptibility of the monkeys to SIV. If the different susceptibilities to SIV (38) correlate with the fact that AGMs are the coexisting natural hosts of SIV and rhesus macaques are the victims, NKT-associated innate immunity may have some relation to those opposite outcomes. Also, the finding that the amino acid sequences of Exon2 and Exon4 corresponding to α_1 and α_3 domains of the CD1d, respectively, were totally identical between the rhesus and AGMs indicates that the domains would be conserved among monkeys, and changes of the amino acid sequences at the sites would destroy the species continuation.

It is widely known that genomic sequences between humans and chimps are highly conserved, and both are susceptible to HIV-1 but very weakly to SIV as reported previously that SIVcpz has been isolated from chimpanzee (39). Thus, we examined the *CD1D* sequence of chimps and determined their consensus sequence for the first time. Interestingly, both α_1 and α_2 domains of the CD1d of chimps were totally identical to humans except for one amino acid at the end of the Exon3; however, three amino acids in Exon4 were distinct from humans, and one of them was the same as identified in the α_3 domain of rhesus macaques and AGMs. In comparison with class I MHC molecules, such α_3 domain of CD1 has been reported to be firmly preserved among each species (20). Moreover, as shown in the Figure 3B, all the crucial amino acids for lipid/glycolipid antigen presentation were strictly conserved among the primates tested, and thus the presented antigens by the α_1 and α_2 domains of CD1d molecule must be the similar among those primates. These results suggest that NKT response to HIV or SIV may not be determined by the antigens presented by the species-specific CD1d molecules, but rather by the structural difference in the CD1d itself or antigen/CD1d complex. Indeed, as shown in Figure 3B, highlighted amino acids at positions Asp(D)151 and Thr(T)154, critical for human NKT-cell activation to the known glycolipid antigens αGalCer (34), were associated with Lys(K)152 and Arg(R)155 in the α_2 domain of the AGM, human, and chimps' CD1d, while they were linked with Asn(N)152 and Lys(K)155 of macaque CD1d, suggesting that distinct susceptibility to SIV may correlate with the CD1d structure and with the activated status of NKT cells because only rhesus macaques fall into immune-deficient state via SIV infection among them.

Taken together, the findings shown in the present study reveal that the α_1 and α_2 domains of the CD1d molecules may present retroviral glycolipid/lipid antigens to the species-specific NKT cells, which may be associated with the type of infectious viruses as well as the susceptibility to them and suggest the evolutionary relationship between the species-specific CD1d molecules and retrovirus infection through the activation of innate effector NKT cells.

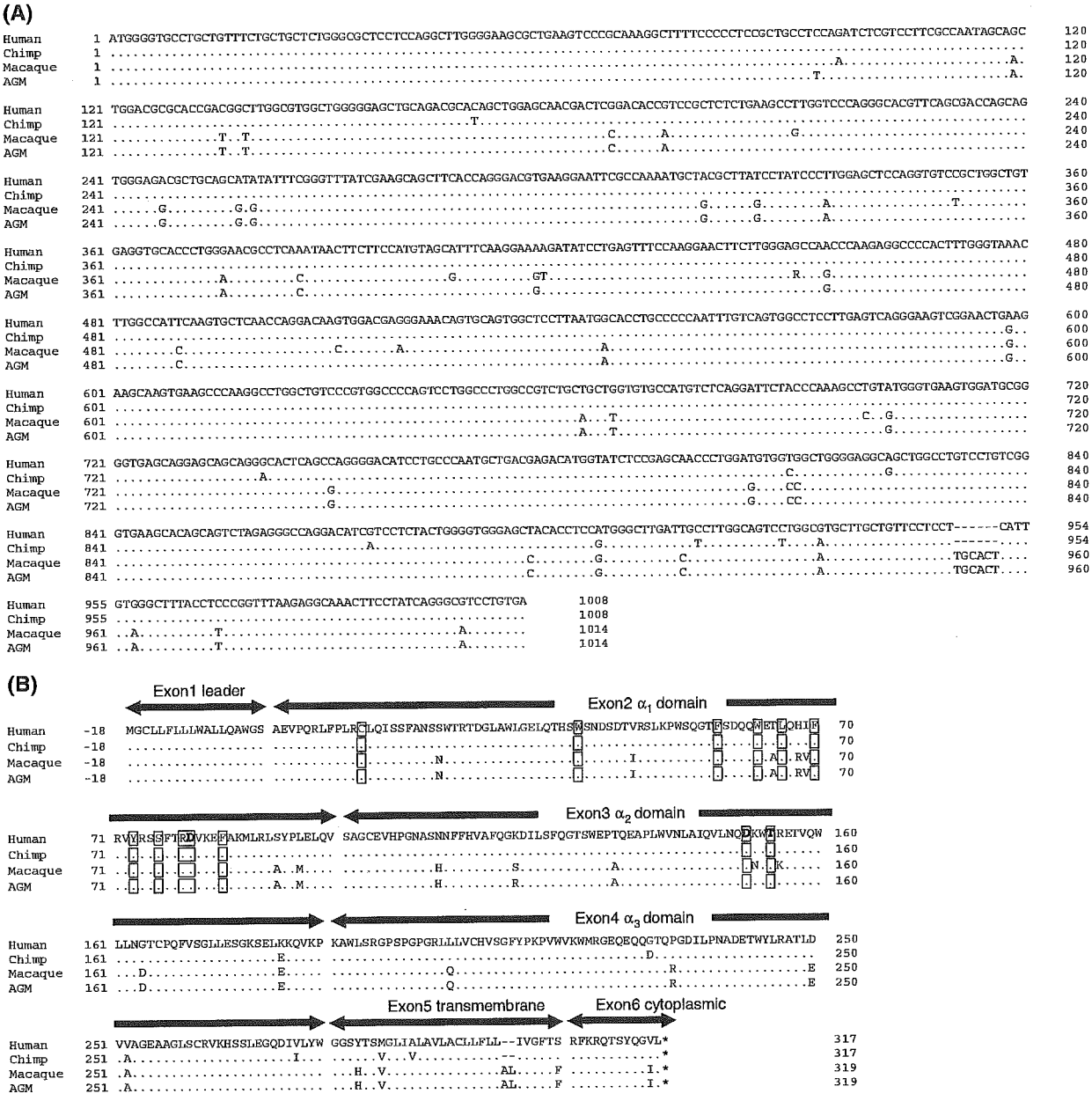

Figures 3 Comparison of consensus *CD1D* sequences between chimpanzees (chimps) and monkeys on the basis of human consensus sequence. (A) Nucleotides alignment of CD1d molecules for each subject. The first line stands for the known human *CD1D*, the second line for the determined chimps' *CD1D*, third line for the rhesus macaques, and the last line for the African green monkeys (AGMs). When the nucleotide was the same with humans, the positions were indicated with dot. (B) Amino acid alignment of CD1d molecules for each subject. Antigen-binding sites, Exon2 and Exon3, were indicated with arrows. Also, the amino acid sequences crucial for antigen presentation were boxed, and those critical for human natural killer T-cell activation among them were highlighted.

Acknowledgments

This work was supported in part by grants from the Ministry of Education, Science, Sport, and Culture, from the Ministry of Health and Labor and Welfare, from the Japanese Health Sciences Foundation, and from the Promotion and Mutual Aid Corporation for Private Schools of Japan.

References

1. Takahashi H. Antigen processing and presentation. *Microbiol Immunol* 1993: **37**: 1–9.
2. Porcelli SA, Segelke BW, Sugita M, Wilson IA, Brenner MB. The CD1 family of lipid antigen-presenting molecules. *Immunol Today* 1998: **19**: 362–8.
3. Takahashi H. Antigen presentation in vaccine development. *Comp Immunol Microbiol Infect Dis* 2003: **26**: 309–28.
4. Nijman HW, Kleijmeer MJ, Ossevoort MA et al. Antigen capture and major histocompatibility class II compartments of freshly isolated and cultured human blood dendritic cells. *J Exp Med* 1995: **182**: 163–74.
5. Burdin N, Kronenberg M. CD1-mediated immune responses to glycolipids. *Curr Opin Immunol* 1999: **11**: 326–31.
6. Brigl M, Brenner MB. CD1: antigen presentation and T cell function. *Annu Rev Immunol* 2004: **22**: 817–90.
7. Gumperz JE, Brenner MB. CD1-specific T cells in microbial immunity. *Curr Opin Immunol* 2001: **13**: 471–8.
8. Moody DB, Young DC, Cheng TY et al. T cell activation by lipopeptide antigens. *Science* 2004: **303**: 527–31.
9. Sieling PA, Chatterjee D, Porcelli SA et al. CD1-restricted T cell recognition of microbial lipoglycan antigens. *Science* 1995: **269**: 227–30.
10. Moody DB, Reinhold BB, Guy MR et al. Structural requirements for glycolipid antigen recognition by CD1b-restricted T cells. *Science* 1997: **278**: 283–6.
11. Beckman EM, Porcelli SA, Morita CT, Behar SM, Furlong ST, Brenner MB. Recognition of a lipid antigen by CD1-restricted alpha beta$^+$ T cells. *Nature* 1994: **372**: 691–4.
12. Moody DB, Ulrichs T, Muhlecker W et al. CD1c-mediated T-cell recognition of isoprenoid glycolipids in *Mycobacterium tuberculosis* infection. *Nature* 2000: **404**: 884–8.
13. Joyce S, Woods AS, Yewdell JW et al. Natural ligand of mouse CD1d1: cellular glycosylphosphatidylinositol. *Science* 1998: **279**: 1541–4.
14. Kawano T, Cui J, Koezuka Y et al. CD1d-restricted and TCR-mediated activation of Valpha14 NKT cells by glycosylceramides. *Science* 1997: **278**: 1626–9.
15. Exley M, Garcia J, Balk SP, Porcelli S. Requirements for CD1d recognition by human invariant Valpha24$^+$ CD4$^-$CD8$^-$ T cells. *J Exp Med* 1997: **186**: 109–20.
16. Bendelac A, Lantz O, Quimby ME, Yewdell JW, Bennink JR, Brutkiewicz RR. CD1 recognition by mouse NK1$^+$ T lymphocytes. *Science* 1995: **268**: 863–5.
17. Jayawardena-Wolf J, Bendelac A. CD1 and lipid antigens: intracellular pathways for antigen presentation. *Curr Opin Immunol* 2001: **13**: 109–13.
18. Couedel C, Peyrat MA, Brossay L et al. Diverse CD1d-restricted reactivity patterns of human T cells bearing 'invariant' AV24BV11 TCR. *Eur J Immunol* 1998: **28**: 4391–7.
19. Matsuura A, Takayama S, Kinebuchi M et al. RT1.P, rat class Ib genes related to mouse TL: evidence that CD1 molecules but not authentic TL antigens are expressed by rat thymus. *Immunogenetics* 1997: **46**: 293–306.
20. Balk SP, Bleicher PA, Terhorst C. Isolation and characterization of a cDNA and gene coding for a fourth CD1 molecule. *Proc Natl Acad Sci USA* 1989: **86**: 252–6.
21. Balk SP, Bleicher PA, Terhorst C. Isolation and expression of cDNA encoding the murine homologues of CD1. *J Immunol* 1991: **146**: 768–74.
22. Katabami S, Matsuura A, Chen HZ, Imai K, Kikuchi K. Structural organization of rat CD1 typifies evolutionarily conserved CD1D class genes. *Immunogenetics* 1998: **48**: 22–31.
23. Kashiwase K, Kikuchi A, Ando Y et al. The CD1d natural killer T-cell antigen presentation pathway is highly conserved between humans and rhesus macaques. *Immunogenetics* 2003: **54**: 776–81.
24. Shinya E, Owaki A, Shimizu M et al. Endogenously expressed HIV-1 nef down-regulates antigen-presenting molecules, not only class I MHC but also CD1a, in immature dendritic cells. *Virology* 2004: **326**: 79–89.
25. Ichikawa M, Sugita M, Takahashi M et al. Breast milk macrophages spontaneously produce granulocyte-macrophage colony-stimulating factor and differentiate into dendritic cells in the presence of exogenous interleukin-4 alone. *Immunology* 2003: **108**: 189–95.
26. Calabi F, Jarvis JM, Martin L, Milstein C. Two classes of CD1 genes. *Eur J Immunol* 1989: **19**: 285–92.
27. Stadler J, Lemmens R, Nyhammar T. Plasmid DNA purification. *J Gene Med* 2004: **6**: S54–66.
28. Zeng Z, Castano AR, Segelke BW, Stura EA, Peterson PA, Wilson IA. Crystal structure of mouse CD1: an MHC-like fold with a large hydrophobic binding groove. *Science* 1997: **277**: 339–45.
29. Beer BE, Bailes E, Goeken R et al. Simian immunodeficiency virus (SIV) from sun-tailed monkeys (*Cercopithecus solatus*): evidence for host-dependent evolution of SIV within the *C. lhoesti* superspecies. *J Virol* 1999: **73**: 7734–44.
30. Puissant B, Abbal M, Blancher A. Polymorphism of human and primate RANTES, CX3CR1, CCR2 and CXCR4 genes with regard to HIV/SIV infection. *Immunogenetics* 2003: **55**: 275–83.
31. Zajonc DM, Cantu C III, Mattner J et al. Structure and function of a potent agonist for the semi-invariant natural killer T cell receptor. *Nat Immunol* 2005: **6**: 810–8.
32. Moody DB, Zajonc DM, Wilson IA. Anatomy of CD1-lipid antigen complexes. *Nat Rev Immunol* 2005: **5**: 387–99.
33. Giabbai B, Sidobre S, Crispin MD et al. Crystal structure of mouse CD1d bound to the self ligand phosphatidylcholine: a molecular basis for NKT cell activation. *J Immunol* 2005: **175**: 977–84.
34. Koch M, Stronge VS, Shepherd D et al. The crystal structure of human CD1d with and without alpha-galactosylceramide. *Nat Immunol* 2005: **6**: 819–26.
35. Kim Y, Nakagawa Y, Sugiyama H et al. Induction of CD4$^+$ murine natural killer T-like cells by immunization with syngeneic thymoma expressing embryonic alpha-fetoprotein. *Cell Immunol* 2003: **226**: 1–10.

36. Kojo S, Adachi Y, Keino H, Taniguchi M, Sumida T. Dysfunction of T cell receptor AV24AJ18$^+$, BV11$^+$ double-negative regulatory natural killer T cells in autoimmune diseases. *Arthritis Rheum* 2001: **44**: 1127–38.
37. Hansen DS, Schofield L. Regulation of immunity and pathogenesis in infectious diseases by CD1d-restricted NKT cells. *Int J Parasitol* 2004: **34**: 15–25.
38. Cranage MP, Cook N, Stott EJ, Cook R, Baskerville A, Greenaway PJ. Transmission studies with simian immunodeficiency virus of macaques; persistent infection of baboons. *Intervirology* 1992: **34**: 53–61.
39. Huet T, Cheynier R, Meyerhans A, Roelants G, Wain-Hobson S. Genetic organization of a chimpanzee lentivirus related to HIV-1. *Nature* 1990: **345**: 356–9.

Arch Virol (2005)
DOI 10.1007/s00705-005-0536-7

Archives of Virology
Printed in Austria

Comparison of susceptibility to SIVmac239 infection between $CD4^+$ and $CD4^+8^+$ T cells

M. Takahashi[1,2], **E. Ido**[3], **H. Uesaka**[2,3], **T. Fukushima**[1,2], **K. Ibuki**[3], **T. Miura**[3], **M. Hayami**[3], and **H. Takahashi**[1,2]

[1]Department of Microbiology and Immunology, Nippon Medical School, Tokyo, Japan
[2]Laboratory of Virus Control, Institute for Virus Research, Kyoto University, Kyoto, Japan
[3]Laboratory of Viral Pathogenesis, Institute for Virus Research, Kyoto University, Kyoto, Japan

Received September 8, 2004; accepted February 17, 2005
Published online April 21, 2005

Summary. CD4-bearing T cells are the primary targets for human immunodeficiency virus type 1(HIV-1)/simian immunodeficiency virus (SIV) infection. However, it is unclear whether the susceptibility of CD4-bearing T cells including CD4 single positive and CD4/8 double positive T cells to HIV/SIV infection is the same or not. In this study, we compared the susceptibility to SIV infection between $CD4^+$ and $CD4^+8^+$ T cells, using Herpesvirus saimiri (HVS)-transformed $CD4^+$ and $CD4^+8^+$ T cells established from peripheral blood mononuclear cells (PBMC) of rhesus macaques. Although there was little difference between the two CD4-bearing T cell population in the expression level of CD4 molecules and chemokine receptors such as CXCR4 and CCR5, SIV replicated more efficiently in $CD4^+8^+$ T cells than in $CD4^+$ T cells. Moreover, we found that reverse transcription initiated more efficiently in $CD4^+8^+$ T cells than in $CD4^+$ T cells and that the cell lysates from $CD4^+$ T cells impaired the RT activity more strongly than that from $CD4^+8^+$ T cells. These findings suggest that intracellular environment in $CD4^+$ 8^+ T cells is better for reverse transcription and that the infection of those $CD4^+8^+$ T cells might play critical and different roles in HIV-1/SIV infection and dissemination.

Introduction

CD4 molecule is the major receptor used by human immunodeficiency virus type 1(HIV-1)/simian immunodeficiency virus (SIV) for binding and entry into target cells. The HIV-1/SIV have a strong cytopathic action on the $CD4^+$ T cells, and the significant depletion of those $CD4^+$ T cells in the blood as well as the peripheral lymphoid organs of infected patients are the hallmarks of progressive immune

impairment leading to AIDS [17, 20]. The chemokine receptors CCR5 and CXCR4 have been identified as co-receptors for HIV-1/SIV [6, 8]. Distribution of these receptors permits the virus to infect to not only $CD4^+$ T cells but also macrophages and dendritic cells (DCs) [7, 12]. After the infection, HIV-1/SIV integrates into the DNA of the host cells. Therefore, the replicating capacity of the integrated viral genome, or provirus, may be greatly influenced by the metabolic and activation state of the host cells [9, 18].

CD4-bearing T cells include both CD4 single positive T cells and CD4/8 double positive T cells. $CD4^+$ T cells broadly distribute in the body, whereas $CD4^+8^+$ T cells are localized in the particular organs such as thymus and small intestine. $CD4^+8^+$ thymocytes, which are situated in the relatively immature stage of differentiation, have been shown a marked susceptibility to HIV-1/SIV infection and replication [3, 22]. Severe depletion of $CD4^+8^+$ T cells in intraepithelial lymphocytes (IELs) was also observed in SIV-infected rhesus macaques [19, 21]. These observations indicate that $CD4^+8^+$ T cells are highly permissive to HIV-1/SIV infection and replication. Thus we speculated that $CD4^+8^+$ T cells might be equally or more susceptible to HIV-1/SIV infection with higher replication capacity in comparison with $CD4^+$ T cells. To address this question, we compared the susceptibility to SIV infection in $CD4^+$ T and $CD4^+8^+$ T cells using Herpesvirus saimiri (HVS)-transformed $CD4^+$ T and $CD4^+8^+$ T cells established from peripheral blood mononuclear cells (PBMC) of rhesus macaques.

Here we show that SIV replicated more efficiently in $CD4^+8^+$ T cells than in $CD4^+$ T cells and such SIV replicating capacity in $CD4^+8^+$ T cells was enhanced via progressed reverse transcription.

Materials and methods

Cell culture and virus

Two $CD4^+$ T cell clones (133, 135-1-3) and two $CD4^+8^+$ T cell clones (135-1, 136-1) were established by HVS-immortalized method [16, 27] from PBMC of three rhesus macaques (*Macaca mulatta*) MM133, MM135 or MM136. Briefly, PBMC were separated from whole blood by Ficoll-Hypaque (Nacalai Tesque, Kyoto, Japan) centrifugation, stimulated for 2 to 3 days with 10 μg/ml of phytohemagglutinin-P (Sigma-Aldrich, St. Louis, MO, USA) and then infected in bulk with HVS strain C-488 (kindly provided by Dr. Yasukawa). After 6 to 8 weeks in culture in RPMI 1640-based medium [25] supplemented with 2 mM L-glutamine, 1 mM sodium pyruvate, 0.1 mM nonessential amino acids, a mixture of vitamins, 1 mM HEPES, 100 U/ml penicillin, 100 μg/ml streptomycin, 50 μM 2-ME, heat-inactivated 10% FCS, and 100 units/ml of human recombinant IL-2, viable cells were recovered by Ficoll-Hypaque separation and $CD4^+$ T cells or $CD4^+8^+$ T cells were cloned by limiting dilution. A molecular clone of SIV (SIVmac239) was used in the present study and was grown on C8166 cells [4] and titrated with M8166 cells (a subclone of C8166). The titer of virus stock was 10^+ $TCID_{50}$/ml.

Infection of $CD4^+$ and $CD4^+8^+$ T cells with SIV

Cells were infected with SIV (moi 0.05-1) in 48 well plates and incubated for 2 h at 37 °C. After washing twice with phosphate buffered saline (PBS) to remove free virus, cells were cultured for 4–7 days.

Reverse transcriptase (RT) assay and detection of p27

The RT assay was performed as described previously [26]. The amount of p27 core antigen in the culture supernatant was measured using the SIV Core Antigen ELISA kit (Beckman Coulter, Fullerton, CA, USA).

Semi-quantitative PCR

DNA was isolated from cultured cells using QIAamp DNA Blood kits (Qiagen, Valencia, CA, USA). Quantification of DNA was performed by real-time PCR with β-actin primers as internal control. Real-time PCR was carried out in a 20 μl containing template DNA, primers for β-actin (forward, 5′-tcacccacactgtgcccatctacga-3′; reverse, 5′-cagcggaaccgctcattgccaatgg-3′), and SYBR Green PCR master mix (Applied Biosystems Foster City, CA, USA). Fluorescence was measured after each cycle using ABI Prism 7700 Sequence Detection System (Applied Biosystems). DNA estimated by real-time PCR was subjected to PCR with the following primers specific for the *nef* gene of SIVmac239 (forward, 5′-ctcactctcttgtgagggacagaaa-3′; reverse, 5′-ccccgtaacatccccttgtggaaagtccc-3′) and the R/U5 region of SIVmac239 LTR (forward, 5′-ttctctccagcactagcaggtagagcctgggtgttccctg-3′; reverse, 5′-caggcgccaatctgcta gggattttcctgcttc-3′). To demonstrate that equal amounts of DNA were subjected to PCR, we showed the electrophoresis data of β-actin PCR product during the exponential phase of amplification.

RNA was prepared from cultured cells using RNAeasy (Qiagen). One microgram of RNA was incubated for 1 h at 42 °C after adding 20 U of RNase inhibitors (Takara, Otsu, Japan), 0.2 mM deoxynucleoside triphosphates, 2.5 nM random primers, 11 U of Rous associated virus 2 reverse transcriptase (Takara) and reverse transcriptase buffer to a final volume of 20 μl. Quantification of cDNA was performed by real-time PCR with β-actin primers as mentioned above. cDNA estimated by real-time PCR was subjected to PCR with the following respective primers specific for CD3 (forward, 5′-tctgctggcctccgccatctt-3′; reverse, 5′-ggagacctgggccagcgggag-3′), CD4 (forward, 5′-ccttcccactcgcctttaca-3′; reverse, 5′-tcagcacccacaccgccttc-3′), Bob (forward, 5′-aaggacagactgtgcatatgtagtctg-3′; reverse, 5′-tcttcagctttttgttgtgctttcctg-3′), and Bonzo (forward, 5′-ggatgacctggggcaaggtcaccagc-3′; reverse, 5′-gtgcttctggaagcctccagcatgaag-3′).

Cell staining

Cells were pelleted and resuspended at a concentration of 5×10^5 cells in 50 μl of PBS with 0.1% NaN_3 containing FITC-labeled mouse anti-CD3 mAb (clone SP34; BD PharMingen, San Diego, CA, USA), PE-labeled mouse anti-CD4 mAb (clone L200; BD PharMingen), FITC-labeled mouse anti-CD8 mAb (clone RPA-T8; BD PharMingen), PE-labeled anti-CXCR4 mAb (clone 12G5; BD PharMingen), or PE-labeled anti-CCR5 mAb (clone 3A9; BD PharMingen). After 30 min incubation on ice, cells were washed and resuspended in PBS for analysis by FACScan (Becton Dickinson, Franklin Lakes, NJ, USA).

Measurement of cell growth

Single cell suspensions were seeded at a density of 1×10^5 cells per well on 96-well microtiter plates. After 7 days of incubation, colorimetric determination of cell growth was performed using XTT Cell Proliferation kit (Roche Diagnostics, Indianapolis, IN, USA).

Virus entry assay

Cells were infected with virus (moi 1) for 2 h at 37 °C. After washing with PBS, cells were treated with 0.05% trypsin containing 0.02% EDTA. After washing extensively, cells were

lysed with lysis buffer (10 mM Tris-HCl (pH 7.5), 10 mM NaCl, 0.5% NP-40). Internalized virion Gag p27 protein was measured using the SIV Core Antigen ELISA kit (Beckman Coulter).

Results

Comparison of viable cell counts after SIV infection

We could successfully establish $CD4^+$ and $CD4^+8^+$ T cell clones from monkey's PBMC by HVS-immortalized method (Fig. 1a). As shown in the right panel of Fig. 1a, the obtained $CD4^+8^+$ T cell clones appeared to contain two subpopulations, $CD4^{high}CD8^{high}$ T cells and $CD4^{high}CD8^{low}$ T cells. It is interesting to note that, when a single cell from either $CD4^{high}CD8^{high}$ or $CD4^{high}CD8^{low}$T cell clones was further cultured, those two promiscuous populations were always emerged. Therefore, the expression level of CD8 molecules on $CD4^+8^+$ T cells might fluctuate. Taking advantage of these $CD4^+$ T cell clones, we then examined their susceptibility to SIVmac239. SIVmac239-infected or uninfected T cells were plated in culture for 7 days and were estimated the viable cell counts by XTT colorimetric method. After 7 days of incubation, a total number of viable cells were significantly decreased in infected $CD4^+8^+$ T cells, whereas that was slightly decreased in infected $CD4^+$ T cells (Fig. 1b).

Assessment of viral replication in $CD4^+$ and $CD4^+8^+$ T cells

To determine viral protein production, the amount of p27 antigens and RT activity in the culture supernatants were measured. The supernatants from SIVmac239-infected $CD4^+8^+$ T cells contained large amounts of p27 antigens

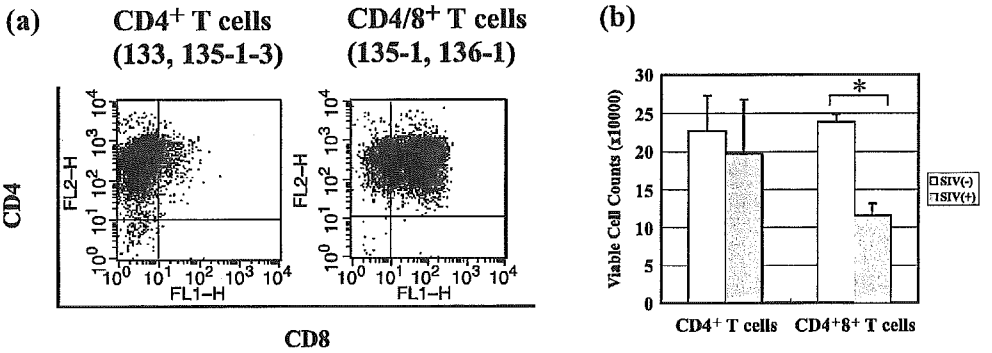

Fig. 1. a HVS-transformed $CD4^+$ and $CD4^+8^+$ T cells established from PBMC of rhesus macaques. Cells were stained with PE-labeled anti-CD4 mAb and FITC-labeled anti-CD8 mAb, followed by propidium iodide staining to exclude dead cells. **b** Determination of viable cell counts in $CD4^+$ and $CD4^+8^+$ T cells after SIV infection. Cells were inoculated with (□) or without (□) SIVmac239 (moi 0.5) and estimated the viable cells by XTT colorimetric method after 7 days incubation. The data shown are the mean of triplicate cultures ±SD (*$P < 0.01$)

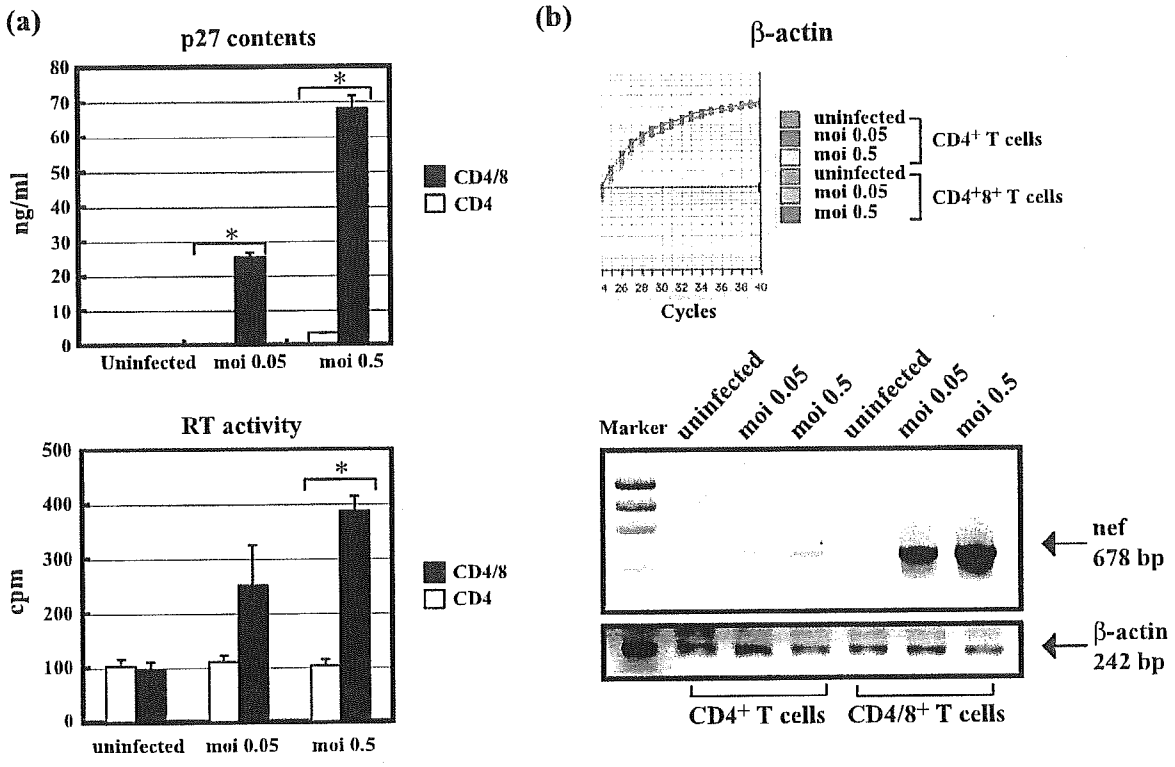

Fig. 2. Assessment of viral replication in $CD4^+$ and $CD4^+8^+$ T cells. $CD4^+$ (□) and $CD4^+8^+$ (■) T cells were infected with SIVmac239 (moi 0.05 or 0.5). After 4 days incubation; **a** the supernatants were harvested and subjected to measure the amount of p27 core antigen and RT activity. The data shown are the mean of triplicate cultures ±SD (*$P < 0.01$). **b** DNA was isolated from infected or uninfected cells and subjected to semi-quantitative PCR using SIVmac239 *nef* or β-actin primer. The thermal cycle was consisted of 30 s at 94 °C, 45 s at 60 °C for *nef* or 55 °C for β-actin, 45 s at 72 °C. The numbers of PCR cycles for *nef* were 35 cycles, and those of β-actin were 24 cycles to generate PCR products during the exponential phase of amplification

and higher level of the RT activity compared to that from infected $CD4^+$ T cells (Fig. 2a). Next, to determine the level of viral DNA synthesis in infected cells, we performed semi-quantitative PCR analysis using the primer pair for the *nef* gene of SIVmac239. As shown in Fig. 2b, low level of the *nef* DNA was detected in infected $CD4^+$ T cells, whereas an evident increase in the *nef* DNA was observed in infected $CD4^+8^+$ T cells.

Effect of SIV infection on CD3 and CD4 expression in $CD4^+$ and $CD4^+8^+$ T cells

It has been reported that HIV/SIV modulated the surface expression of various molecules [11]. Therefore, we analyzed the expression level of surface CD3 and CD4 molecules on both SIVmac239-infected $CD4^+$ and $CD4^+8^+$ T cells by

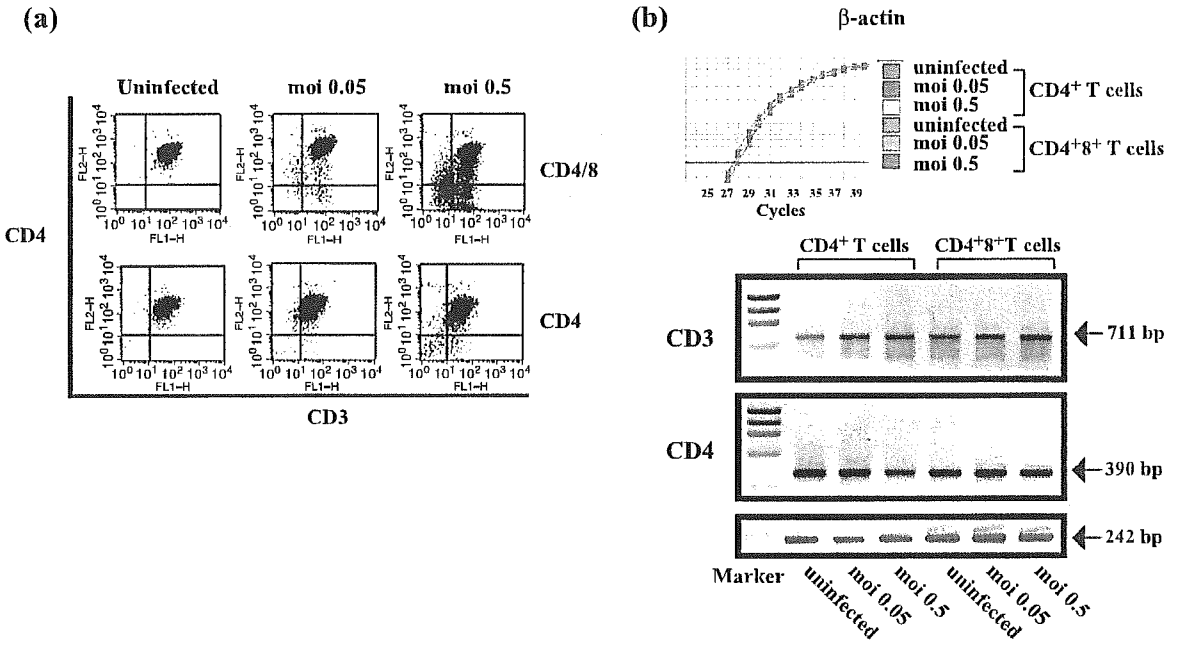

Fig. 3. Effect of SIVmac239 infection on CD3 and CD4 expression on $CD4^+$ and $CD4^+8^+$ T cells. $CD4^+$ and $CD4^+8^+$ T cells were infected with SIV (moi 0.05 or 0.5). After 4 days incubation; **a** Cells were stained with FITC-labeled anti-CD3 mAb and PE-labeled anti-CD4 mAb, followed by propidium iodide staining to exclude dead cells. **b** RNA was isolated from infected or uninfected cells and then reverse-transcribed into cDNA. cDNA was subjected to semi-quantitative PCR using CD3, CD4 or β-actin primer. The thermal cycle was consisted of 30 s at 94 °C, 45 s at 60 °C for CD3 and CD4, or 55 °C for β-actin, 45 s at 72 °C. The numbers of PCR cycles for CD3 and CD4 were 33 cycles, and those of β-actin were 24 cycles to generate PCR products during the exponential phase of amplification

flow cytometry. SIV-infected $CD4^+8^+$ T cells showed marked down-modulation for both CD3 and CD4 expression when compared with infected $CD4^+$ T cells (Fig. 3a). The down-modulation was dependent on the infectious doses of virus. Since semi-quantitative RT-PCR analysis demonstrated that the respective levels of CD3 and CD4 transcripts did not change between uninfected and infected cells, down-modulation is due to the internalization of these molecules induced by the virus infection (Fig. 3b).

Evaluation of receptor and co-receptor expression on $CD4^+$ and $CD4^+8^+$ T cells and virus entry

Since efficiency of SIV entry depends on the presence of appropriate receptor and co-receptor, we examined the expression levels of those receptors on uninfected $CD4^+$ T cells or $CD4^+8^+$ T cells by FACS and RT-PCR analysis. There seemed little difference in the expression levels of CD4, CXCR4 or CCR5. The transcript level of Bob was almost the same, whereas that of Bonzo was slightly decreased